COMPRESSIVE SAMPLING FOR NON-INTRUSIVE APPLIANCE LOAD MONITORING (NALM) USING CURRENT WAVEFORMS

Ying Wang, Alessio Filippi, Ronald Rietman
Philips Research,
Eindhoven, The Netherlands
email: {ying.z.wang, alessio.filippi, ronald.rietman}
@philips.com

Geert Leus
Department of EEMCS,
Delft University of Technology,
Delft, The Netherlands
email: g.j.t.leus@tudelft.nl

ABSTRACT

We propose a NALM technique by exploiting the compressive sampling and sparse reconstruction framework. We estimate the contribution of the individual appliances by measuring the current of the total load. We further assume to know the steady-state current waveform of each appliance. We exploit the sparsity of the current signal to compress the measurement via random sampling, which lowers significantly the processing complexity, the storage and the communication burden. Using the proposed sparse reconstruction approach, we can still identify the on/off status of each appliance from the compressed measurement as if the original non-compressed measurement is used.

KEY WORDS

Estimation of Signal Parameters, Compressive Sampling.

1 Introduction

Energy consumption monitoring is a key aspect in achieving sustainable development. Advanced monitoring techniques are desired to obtain fine-grained (e.g., down to individual electrical appliance in a home), real-time and reliable energy consumption information. Such information can provide insights to impact the consumers positively on energy conservation, and can also enable utility companies to offer advanced services like dynamic electricity pricing. The non-intrusive appliance load monitoring (NALM) [1] is a convenient approach to determine the energy consumption of individual appliances. The NALM employs only a single point of measurement, e.g., at the main electrical service entry point of the home, which does not require installing meters on each individual appliance. The NALM monitors the voltage and current of the total load and derives the activity of the individual appliances which constitute the load. Each appliance has electrical features that can be used as a unique 'signature' to recognize its contribution in the overall consumption. The most well developed NALM technique utilizes the signature given by the real and reactive power of the appliance during its steady-state operation (i.e., excluding a short duration of the off-to-on transient state) [1]. To resolve the ambiguity when two appliances have the same power signatures, more advanced techniques are proposed which exploit other signatures, including the steady-state current waveform [5], the transient-state current waveform [3], etc.

The current signature based approaches rely on the high frequency components to make the appliance more unique/distinguishable, which typically require a higher sampling rate (e.g., 40 kHz in [3]) than the power signature based approaches (e.g., 2-10 Hz in [1]). Compressive sampling (CS) is a method of acquiring and reconstructing sparse signals [2]. One particular CS application of interest here is the analog-to-information convertor (AIC) [4] that can sample below the Nyquist-rate required by the conventional analog-to-digital convertor (ADC).

In this paper, we will propose a steady-state current signature based NALM method that utilizes compressive sampling and sparse reconstruction techniques. By exploiting the sparsity in terms of the on/off status of the appliances, we can compress the measured current signal with AIC sampling, while still achieving reliable appliance identification from the compressed measurements. The rest of this paper is organized as follows. In Section 2 we present the signal model and propose the measurement methods and the disaggregation algorithms for recognizing the individual appliance usage. We conducted experiments to verify the proposed NALM solution as discussed in Section 3. The performance is evaluated by simulations in Section 4. Conclusions are drawn in Section 5.

2 Our Approach

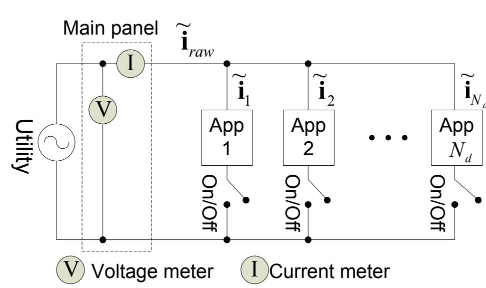

Figure 1. Electrical circuit model of a household.

The electrical circuit model of a household is depicted in Figure 1, where multiple appliances are connected as N_d

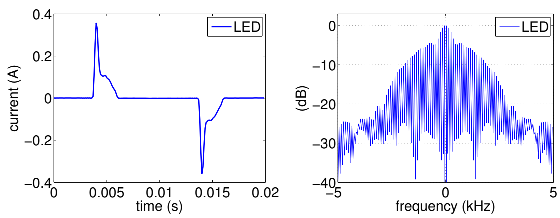

(a) time domain (b) frequency domain

Figure 2. An example: one period of the steady-state current drawn by an LED light bulb.

parallel loads that switch on and off independently. We place a voltage meter and a current meter at a central monitoring point, e.g., the main electric panel of a home. The voltage meter measures the source voltage delivered by the utility, which is a sinusoidal wave of 50 Hz (in Europe). When the d-th ($d = 1, 2, \ldots, N_d$) appliance load is turned on, it draws the current signal denoted as $\tilde{\mathbf{i}}_d$ during steady state. The steady-state current waveform has several properties: 1) repeatable with the fundamental period of 1/50 s, 2) unique so that it can be used as the load's signature, and 3) additive if multiple loads are 'on'. The current meter measures $\tilde{\mathbf{i}}_{raw}$, i.e., the current signal drawn by the total load, which is the sum of the $\tilde{\mathbf{i}}_d$'s of the 'on' loads.

Using the measured voltage and current of the total load in a steady state, we perform a disaggregation algorithm to obtain the individual appliance usage information. The steady-state current waveform of each appliance can be measured individually off-line, which constitutes a signature database for on-line appliance identification. An example of the steady-state current drawn by an LED light bulb is given in Figure 2, where (a) is the time domain waveform of one period, and (b) is the frequency domain spectrum (i.e., the Fourier transform of the time domain waveform). Let F_s denote the Nyquist-rate of the current signal, which is defined as the bandwidth of the spectral components satisfying a threshold, e.g., $<$ 30 dB below the peak spectrum. Then the spectrum in (b) suggests that the Nyquist-rate of the current signal is $F_s = 10$ kHz.

One period ($T = 1/50$ s) of the current signal contains $N = TF_s$ Nyquist-rate samples. The current signal of the d-th appliance is expressed by an $N \times 1$ vector (for one period),

$$\tilde{\mathbf{i}}_d = A_d \mathbf{i}_d, \tag{1}$$

where $\mathbf{i}_d$ is normalized s.t. $\mathbf{i}_d^H \mathbf{i}_d = 1$ and A_d is the amplitude. The Nyquist-rate digital signal representation of (1) is conceptually viewed as the raw analog current signal.

2.1 Pre-filtering

Before analog-to-digital conversion, we apply pre-filtering to improve the signal condition for later processing. The filtered version of (1) is

$$\tilde{\mathbf{u}}_d = W\{\tilde{\mathbf{i}}_d\} = B_d \mathbf{u}_d, \tag{2}$$

where $W\{\cdot\}$ represents the pre-filter (without changing the length of $\tilde{\mathbf{i}}_d$), $\mathbf{u}_d$ is normalized s.t. $\mathbf{u}_d^H \mathbf{u}_d = 1$, and B_d is the amplitude. Generally, $W\{\cdot\}$ can be any filter or transform designed to enhance the signal dynamic range for ADC sampling, and/or to reduce the signal correlations for disaggregation. In the remainder of this paper, we use (2) as a general expression for the current signal, which includes (1) as a special case, i.e., when $W\{\tilde{\mathbf{i}}_d\} = \mathbf{I}_N \tilde{\mathbf{i}}_d$ ($\mathbf{I}_N$ is an $N \times N$ identity matrix), $\mathbf{u}_d = \mathbf{i}_d$ and $B_d = A_d$.

We define a basis matrix of size $N \times N_d$ as

$$\mathbf{\Psi} = [\mathbf{u}_1 \ \mathbf{u}_2 \ \cdots \ \mathbf{u}_{N_d}]. \tag{3}$$

Ignoring the additive noise term, the measured current is

$$\tilde{\mathbf{i}} = W\{\tilde{\mathbf{i}}_{raw}\} = W\{\sum_{d=1}^{N_d} \tilde{\mathbf{i}}_d s_d\} = \sum_{d=1}^{N_d} \tilde{\mathbf{u}}_d s_d = \mathbf{\Psi}\mathbf{B}\mathbf{s}, \tag{4}$$

where $\mathbf{B} = diag[B_1 \ B_2 \ \cdots \ B_{N_d}]$ is a diagonal matrix, and $\mathbf{s}$ is an $N_d \times 1$ status signal vector, with elements s_d equal to 0 or 1 indicating the on or off status of the d-th appliance. Note that (4) represents conceptually the analog current signal before the ADC, with a bandwidth of F_s Hz.

2.2 Sparsity of the Status Signal

We say that the status signal $\mathbf{s}$ is K_0-sparse if it contains only K_0 ($K_0 \ll N_d$) non-zero entries, by assuming that at a steady state, only a small number of appliances are simultaneously 'on'. If $\mathbf{s}$ is not sparse, a new sparse signal can be introduced based on the switch continuity principle (SCP) [1], i.e., in a short time interval only a small number of appliances are expected to change their status. Denoting τ as the time instant when (4) is observed, we can write

$$\tilde{\mathbf{i}}_\tau = \mathbf{\Psi}\mathbf{B}\mathbf{s}_\tau, \tag{5}$$

where $\mathbf{s}_\tau$ is the status signal at the time instant τ. Let τ_1, τ_2 be two time instants respectively before and after certain status changes of appliances, and $\tau_2 - \tau_1$ be a small time interval within which only K_0 ($K_0 \ll N_d$) appliances change their status. We obtain the difference signal as

$$\tilde{\mathbf{i}}' = \tilde{\mathbf{i}}_{\tau_2} - \tilde{\mathbf{i}}_{\tau_1} = \mathbf{\Psi}\mathbf{B}\mathbf{s}', \tag{6}$$

where $\mathbf{s}' = \mathbf{s}_{\tau_2} - \mathbf{s}_{\tau_1}$ contains the change-of-status information of the N_d appliances. The element of $\mathbf{s}'$ can take one of the three values, 0 (no status change), 1 (off to on), and -1 (on to off). Even if none of $\mathbf{s}_{\tau_1}$ or $\mathbf{s}_{\tau_2}$ is sparse, $\mathbf{s}'$ is K_0-sparse given the SCP.

2.3 Compressed Measurements/Samples

We define a measurement/sampling matrix $\mathbf{\Phi}$ of size $M \times N$ ($M \le N$), which converts the analog signal $\tilde{\mathbf{i}}$ to the digital signal $\mathbf{i}_{\mathrm{m}}$,

$$\mathbf{i}_{\mathrm{m}} = \mathbf{\Phi}\tilde{\mathbf{i}} = \mathbf{\Psi}_{\mathrm{m}}\mathbf{B}\mathbf{s}. \tag{7}$$

A new basis matrix $\mathbf{\Psi}_\mathrm{m}$ is given by

$$\mathbf{\Psi}_\mathrm{m} = \mathbf{\Phi}\mathbf{\Psi} = [\mathbf{m}_1\ \mathbf{m}_2\ \cdots \mathbf{m}_{N_d}], \tag{8}$$

where $\mathbf{m}_d = \mathbf{\Phi}\mathbf{u}_d$ is the basis vector of the measured/sampled signal. The matrix $\mathbf{\Phi}$ can represent both the conventional ADC sampling and the compressive AIC sampling, i.e.,

1. Non-compressed: If $M = N$ and $\mathbf{\Phi} = \mathbf{I}_N$, then $\mathbf{\Phi}$ represents the conventional sampling with an ADC running at F_s Hz.
2. Compressed: If $M < N$ and $\mathbf{\Phi}$ contains elements drawn randomly from a distribution (e.g. Gaussian), then $\mathbf{\Phi}$ represents compressive sampling with an AIC running at $(M/N)F_s$ Hz. Knowing that $\mathbf{s}$ (or $\mathbf{s}'$) is K_0-sparse as discussed in Section 2.2, we can use a random and non-adaptive matrix $\mathbf{\Phi}$ to compress $\tilde{\mathbf{i}}$ (or $\tilde{\mathbf{i}}'$) to only $M = \mathcal{O}(K_0 \ln N_d)$ samples [2], from which a reliable estimation of $\mathbf{s}$ (or $\mathbf{s}'$) can still be achieved.

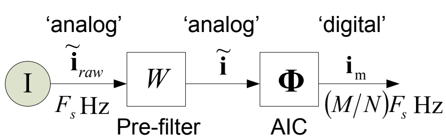

Figure 3. The measurement process.

The measurement process is summarized in Figure 3. In practice the AIC sampling described by (7) is implemented using analog circuits, where the multiplication of $\mathbf{\Phi}$ and $\tilde{\mathbf{i}}$ is performed using mixers and integrators [4]. The compressed measurement $\mathbf{i}_\mathrm{m}$ is used for further digital signal processing, e.g., performing a disaggregation algorithm to derive the individual appliance usage information. The $\mathbf{i}_\mathrm{m}$ can be either processed by a local microprocessor attached to the meter or sent to a remote PC if the meter is equipped with a wireless communication module. The compression lowers both the processing complexity and the communication burden.

2.4 Disaggregation Algorithm

Given $\mathbf{\Psi}_\mathrm{m}$ and $\mathbf{B}$ as the known appliance signature, we want to estimate the status signal $\mathbf{s}$ based on the measured signal $\mathbf{i}_\mathrm{m}$. Rewrite (7) as

$$\mathbf{i}_\mathrm{m} = \mathbf{\Psi}_\mathrm{m}\mathbf{z}, \tag{9}$$

where $\mathbf{z} = \mathbf{B}\mathbf{s}$ is the status signal weighted by the amplitudes. One straightforward solution of $\mathbf{z}$ can be obtained via the least-squares (LS) estimate,

$$\hat{\mathbf{z}} = \mathbf{\Psi}_\mathrm{m}^\dagger \mathbf{i}_\mathrm{m}, \tag{10}$$

where † denotes the Moore-Penrose pseudoinverse of a matrix. The LS minimizes the l_2-norm and suffers from overestimation when the solution is sparse. As discussed in Section 2.2, $\mathbf{z}$ is sparse (or using the difference signal formulation of (6), $\mathbf{z}' = \mathbf{B}\mathbf{s}'$ is sparse). It is better to employ the l_1-norm minimization approach, i.e.,

$$\hat{\mathbf{z}} = \arg\min_{\mathbf{z}} \|\mathbf{z}\|_1 \quad \text{s.t.} \quad \mathbf{i}_\mathrm{m} = \mathbf{\Psi}_\mathrm{m}\mathbf{z}. \tag{11}$$

The optimization problem of (11) can be solved by greedy pursuit algorithms such as orthogonal matching pursuit (OMP) [6]. We will present two algorithms, the appliance matching pursuit (A-MP) in Table 1 and the appliance orthogonal matching pursuit (A-OMP) in Table 2, by adapting the original OMP algorithm to our settings for appliance identification. *Notation*: $\mathbf{\Omega} = \{1, 2, \ldots, N_d\}$ is the index set of all the appliances. $\mathbf{\Omega}_K = \{d_1, d_2, \ldots, d_K\} \subseteq \mathbf{\Omega}$ is the index set of the 'on' appliances selected by the algorithms.

A-MP has less computational complexity than A-OMP, since A-OMP performs matrix multiplication in the orthogonalization step of each iteration and also needs more iterations to converge. A-OMP is more robust than A-MP when the appliance signature waveforms are very correlated.

Given $\mathbf{\Omega}_K$, we obtain a mutilated basis matrix $\mathbf{\Psi}_{\mathrm{m},K} = [\mathbf{m}_{d_1}\ \mathbf{m}_{d_2}\ \cdots\ \mathbf{m}_{d_K}]$, and a mutilated coefficient vector $\mathbf{z}_K = [z_{d_1}\ z_{d_2}\ \cdots\ z_{d_K}]^T$, such that (9) can be rewritten as $\mathbf{i}_\mathrm{m} = \mathbf{\Psi}_{\mathrm{m},K}\mathbf{z}_K$. Then $\mathbf{z}_K$ is estimated by

$$\hat{\mathbf{z}}_K = \mathbf{\Psi}_{\mathrm{m},K}^\dagger \mathbf{i}_\mathrm{m}. \tag{12}$$

Similarly, a mutilated status signal vector is defined as $\mathbf{s}_K = [s_{d_1}\ s_{d_2}\ \cdots s_{d_K}]^T$. Knowing the amplitudes, we estimate $\mathbf{s}_K$ and obtain a refined index set as

$$\hat{s}_{d_k} = \hat{z}_{d_k}/B_{d_k}, \quad d_k \in \mathbf{\Omega}_K, \tag{13}$$

$$\mathbf{\Omega}_{K^*} = \{d_k : \hat{s}_{d_k} > 0.5\}, \tag{14}$$

where the threshold is set to be 0.5, given that the status signal is either 0 or 1 with equal probability.

3 Experiments

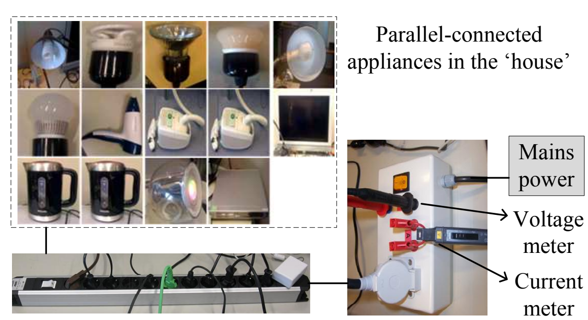

Figure 4. Experimental set-up.

We built an experimental set-up as shown in Figure 4 to emulate an NALM system with some household appliances including different types of lamps, vacuum cleaner,

Table 1. A-MP algorithm

Input: $\mathbf{i}_\mathrm{m}$, $\mathbf{\Psi}_\mathrm{m}$, $\mathbf{B}$, and thresholds α, ϵ.
Initialize: the residual $\mathbf{r}_0 = \mathbf{i}_\mathrm{m}$, the index set $\mathbf{\Omega}_0 = \emptyset$.
Iterate: the k-th iteration, $k = 1, 2, \ldots$

1. Select some candidate appliances

$$\begin{aligned} \rho_d &= \mathbf{r}_{k-1}^H \mathbf{m}_d / \|\mathbf{m}_d\|, \\ C &= \{d : \rho_d \geq \alpha \max \rho_d\}, \quad d \in \mathbf{\Omega} \setminus \mathbf{\Omega}^{k-1}. \end{aligned}$$

2. From the candidate set C, select the one appliance that minimizes the residual power

$$\begin{aligned} d_k &= \arg\min_{d \in C} \|\mathbf{r}_{k-1} - B_d \mathbf{m}_d\|, \\ \mathbf{\Omega}_k &= \mathbf{\Omega}_{k-1} \cup \{d_k\}. \end{aligned}$$

3. Update the residual

$$\begin{aligned} \mathbf{r}_k &= \mathbf{r}_{k-1} - B_{d_k} \mathbf{m}_{d_k}, \\ e_k &= (\|\mathbf{r}_{k-1}\|^2 - \|\mathbf{r}_k\|^2) / \|\mathbf{r}_{k-1}\|^2. \end{aligned}$$

Stop criteria: If $e_k < \epsilon$ or $k = N_d$.
Output: $\mathbf{\Omega}_K$ (stop after K iterations).

Table 2. A-OMP algorithm

Input: $\mathbf{i}_\mathrm{m}$, $\mathbf{\Psi}_\mathrm{m}$, and a threshold ϵ.
Initialize: the residual $\mathbf{r}_0 = \mathbf{i}_\mathrm{m}$, the index set $\mathbf{\Omega}_0 = \emptyset$, the matrix containing the orthogonalized selected basis vectors $\mathbf{\Gamma}_0 = [\,]$.
Iterate: the k-th iteration, $k = 1, 2, \ldots$

1. Select one appliance and add to the index set

$$\begin{aligned} \rho_d &= \mathbf{r}_{k-1}^H \mathbf{m}_d / \|\mathbf{m}_d\|, \\ d_k &= \arg \max_{d \in 1, \ldots, N_d} \rho_d, \quad \mathbf{\Omega}_k = \mathbf{\Omega}_{k-1} \cup \{d_k\}. \end{aligned}$$

2. Orthogonalize and normalize the selected basis vector, and add it to the orthogonalized basis matrix

$$\begin{aligned} \tilde{\mathbf{m}}_{d_k} &= \mathbf{m}_{d_k} - \mathbf{\Gamma}_{k-1} \mathbf{\Gamma}_{k-1}^H \mathbf{m}_{d_k}, \\ \mathbf{g}_k &= \tilde{\mathbf{m}}_{d_k} / \|\tilde{\mathbf{m}}_{d_k}\|, \\ \mathbf{\Gamma}_k &= [\mathbf{\Gamma}_{k-1}\ \mathbf{g}_k]. \end{aligned}$$

3. Update the residual

$$\begin{aligned} \mathbf{r}_k &= \mathbf{r}_{k-1} - (\mathbf{r}_{k-1}^H \mathbf{g}_k) \mathbf{g}_k, \\ e_k &= (\|\mathbf{r}_{k-1}\|^2 - \|\mathbf{r}_k\|^2) / \|\mathbf{r}_{k-1}\|^2. \end{aligned}$$

Stop criteria: If $e_k < \epsilon$ or $k = N_d$.
Output: $\mathbf{\Omega}_K$ (stop after K iterations).

TV, DVD player, hair dryer, and kettle. The set-up is fed by mains power that behaves as a service entry point delivering electricity to the 'house'. The sensing box is equipped with a current meter measuring the overall current and a voltage meter measuring the mains voltage. The current meter is an Agilent current probe placed around the single core of the live or neutral wire. The voltage meter is a differential voltage probe, which in principle can be put at any socket in the 'house'. Usually each appliance has one steady-state current waveform as its unique signature. For some multi-mode appliances (e.g., standby/cooking for the kettle, low/high-power for the vacuum cleaner), each operation mode has a unique steady-state current waveform counted as a signature. In our case, there are 12 appliances with $N_d = 14$ signatures. The signal from the current probe is sampled by a 24-bit ADC running at $F_s = 10$ kHz, which is the suggested Nyquist rate as discussed in Section 2. Given the high enough ADC sampling rate, the digitized signal is conceptually viewed as the 'analog' signal, based on which we emulate the pre-filter $W\{\cdot\}$ and the AIC $\mathbf{\Phi}$ in digital domain.

3.1 Appliance Signatures

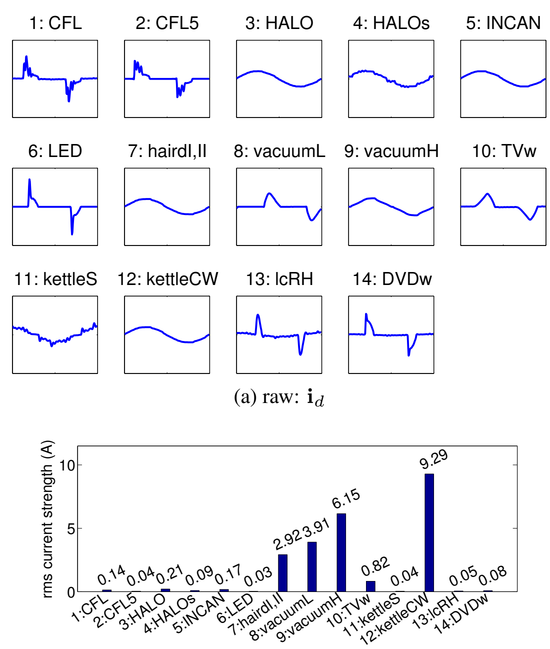

(a) raw: $\mathbf{i}_d$

(b) raw: $A_d/\sqrt{N}$

Figure 5. Appliance signatures (raw signal).

The signature database is obtained by measuring the current waveform of each appliance (or operation mode) individually. In the future, self-learning algorithms can be designed to build the signature database automatically when an un-registered appliance is plugged in. The raw current signatures (without pre-filtering) are shown in Figure 5, where (5a) is $\mathbf{i}_d$ describing the current shape, and (5b) is $A_d/\sqrt{N}$ describing the root-mean-square (rms) current strength in Amperes. The 14 signatures are named and numbered according to the appliances in Figure 4. As shown in (5a), different loads produce different current shapes, while certain loads with similar circuit characteristics produce very similar current shapes, e.g., the resistive loads including hair dryer, kettle (cooking mode), halogen lamp, and incandescent lamp all having a sinusoidal current shape. We observe from (5b) that the current strength ranges from 0.03 A to 9.29 A.

3.2 Effects of Pre-filtering

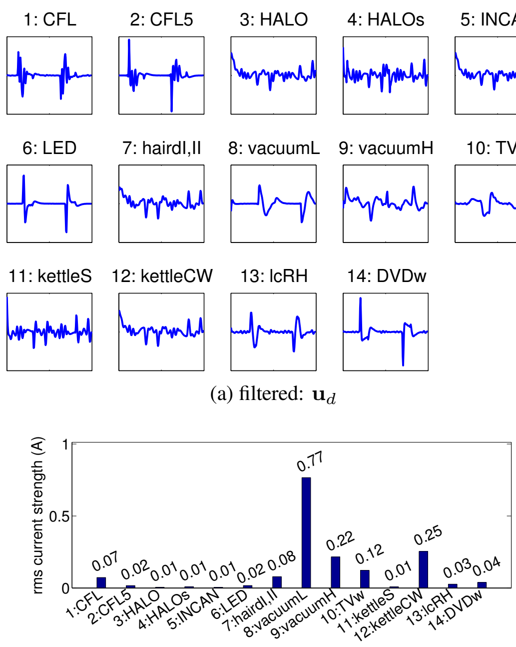

(a) filtered: $\mathbf{u}_d$

(b) filtered: $B_d/\sqrt{N}$

Figure 6. Appliance signatures (notch-filtered signal).

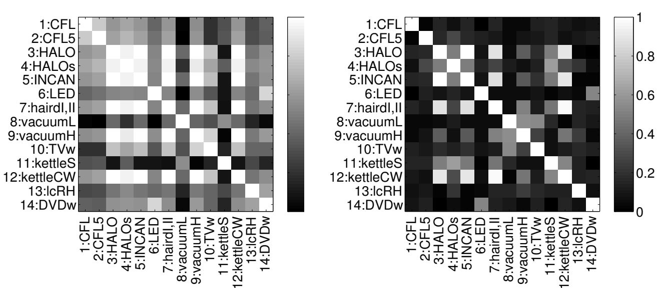

(a) raw: $\mathbf{R_i}$

(b) filtered: $\mathbf{R_u}$

Figure 7. Appliance signature correlations.

The $W\{\cdot\}$ we use is a notch filter removing the ± 50 Hz components of the raw signal, with the transfer function of $H(z) = (1 - 2\cos\omega_0 z^{-1} + z^{-2})/(1 - 2r\cos\omega_0 z^{-1} + r^2 z^{-2})$, where $\omega_0 = 2\pi 50/F_s$ and $r = 0.8$ is a parameter $(0 < r < 1)$ controlling the width of the notch. The signatures of the filtered current are shown in Figure 6. Without the 50 Hz components, the higher order harmonics become more dominant and the current shapes become more fluctuating as shown in (6a). The filtered current strength ranges from 0.01 A to 0.77 A as shown in (6b), which decreases a lot as compared to (5b). We describe the similarity between the two current shapes (indexed by d_1 and d_2) by calculating the correlation as $\mathbf{R_i}(d_1, d_2) = \mathbf{i}_{d_1}^H \mathbf{i}_{d_2}$ for the raw signal, and $\mathbf{R_u}(d_1, d_2) = \mathbf{u}_{d_1}^H \mathbf{u}_{d_2}$ for the filtered signal. Figure 7 shows the result correlations by color, where the whiter the more correlated and the darker the less. The signature correlations decrease significantly after notch-filtering, which will assist the disaggregation.

3.3 Measurement

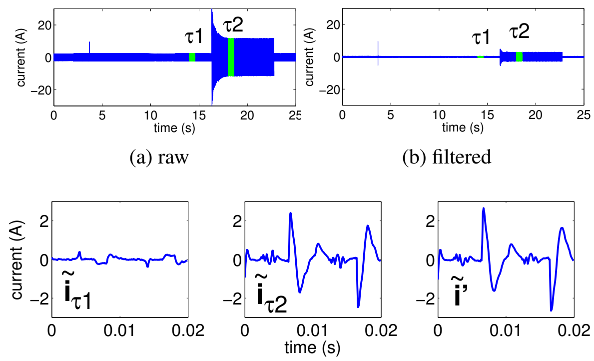

(a) raw

(b) filtered

(c) filtered

Figure 8. The measured current signal (without compression). 'On': [4 6 10 14] at τ_1; [1 2 4 6 8 10 13 14] at τ_2.

We measure the overall current over 25 s, during which some appliances are turned on sequentially and some are turned on simultaneously. Figure 8 shows the measured current (without compression), where (8a) is the raw signal and (8b) is the notch-filtered signal. Within the 25 s, there are two highlighted short segments with a duration of 0.6 s each, denoted by τ_1 and τ_2 respectively. The segment τ_1 contains the steady-state measurement where the appliances indexed by [4 6 10 14] are 'on'. In between τ_1 and τ_2, some appliances ([1 2 8 13]) are turned on simultaneously, and the segment τ_2 contains the steady-state measurement where the appliances [1 2 4 6 8 10 13 14] are all 'on'. Averaging over the 30 periods (0.6 s) in each segment, we obtain the waveform of one period (0.02 s), denoted as $\tilde{\mathbf{i}}_{\tau_1}$ and $\tilde{\mathbf{i}}_{\tau_2}$ for the segments τ_1 and τ_2 respectively. The difference waveform $\tilde{\mathbf{i}}'$ is given by $\tilde{\mathbf{i}}_{\tau 2} - \tilde{\mathbf{i}}_{\tau 1}$. The $\tilde{\mathbf{i}}_{\tau_1}$, $\tilde{\mathbf{i}}_{\tau_2}$ and $\tilde{\mathbf{i}}'$ of the notch-filtered signal are shown in (8c), based on which we will test our disaggregation algorithms.

3.4 The Proposed Algorithms

We test the disaggregation algorithms using the filtered measurement $\tilde{\mathbf{i}}_{\tau_1}$, where the 'on' appliances are [4 6 10 14]

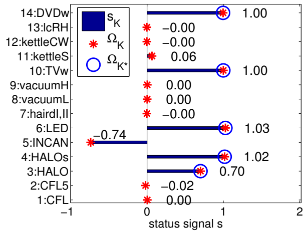

(a) LS, 3 (HALO) over-estimated

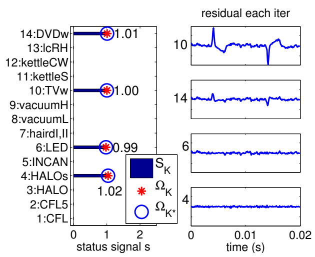

(b) A-MP, correct

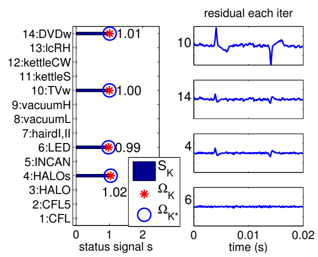

(c) A-OMP, correct

Figure 9. Appliance identification results. Measurement $\tilde{\mathbf{i}}_{\tau_1}$ with [4 6 10 14] 'on'.

as mentioned in Section 3.3. The threshold values for the A-MP and A-OMP are $\alpha = 0.9$ and $\epsilon = 0.05$. The appliance identification results are shown in Figure 9, where (9a) uses the conventional LS algorithm, and (9b) and (9c) use the two proposed algorithms. In the figures, the bar denotes the estimated status signal $\hat{\mathbf{s}}_K$, the $*$ denotes the index set $\boldsymbol{\Omega}_K$, and the $\circ$ denotes the refined index set $\boldsymbol{\Omega}_{K^*}$. For LS, $\boldsymbol{\Omega}_K = \boldsymbol{\Omega}$ and $\hat{\mathbf{z}}_K = \hat{\mathbf{z}}$ of (10). For A-MP and A-OMP, we also plot the residual signal of each iteration to illustrate how the iterative procedure converges, where the number on the y-label is the selected appliance index of that iteration. As shown in (9a), the LS identifies the 'on' appliances to be [3 4 6 10 14], where the appliance 3 (HALO) is wrongly identified to be 'on', i.e., over-estimated. As shown in (9b) and (9c), both A-MP and A-OMP correctly identify the 'on' appliances to be [4 6 10 14].

3.5 The Effects of Compression

We test compression using the difference waveform $\tilde{\mathbf{i}}'$, which in effect contains the 'on' appliances indexed by [1 2 8 13] as mentioned in Section 3.3. The non-compressed signal $\tilde{\mathbf{i}}'$ is sampled at 10 kHz (the Nyquist-rate) giving $N = 200$ samples. The compressed signal $\mathbf{i}'_{\mathrm{m}}$ is sampled at 1 kHz (1/10 of the Nyquist-rate) giving $M = 20$ samples. We consider four sampling matrices as shown in Figure (10a) with $\mathbf{\Phi}$'s coefficients displayed as colors: 1) **Nyquist** - Nyquist-rate sampling, where $\mathbf{\Phi} = \mathbf{I}_N$; 2) **subs** - conventional sub-sampling, where $\mathbf{\Phi}$ is obtained by taking one out of every N/M rows from $\mathbf{I}_N$; 3) **randg** - random Gaussian compressive sampling, where $\mathbf{\Phi}$ contains $M \times N$ elements drawn i.i.d. from a random Gaussian distribution with zero mean and variance $1/M$; 4) **rands** - random selection compressive sampling, where $\mathbf{\Phi}$ is obtained by taking randomly M rows from $\mathbf{I}_N$. Figure (10b) shows the current signal sampled by the four $\mathbf{\Phi}$'s.

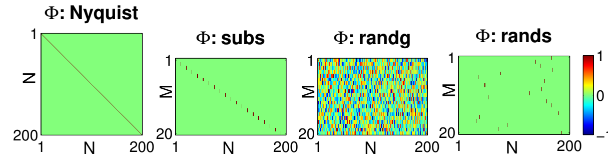

(a) sampling matrix $\mathbf{\Phi}$

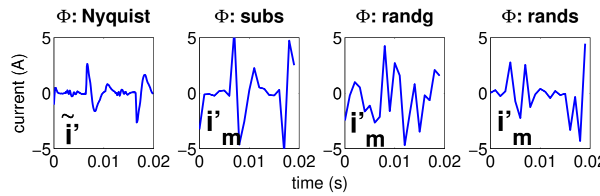

(b) sampled current signal

Figure 10. The $\tilde{\mathbf{i}}'$ sampled/compressed by different $\mathbf{\Phi}$'s.

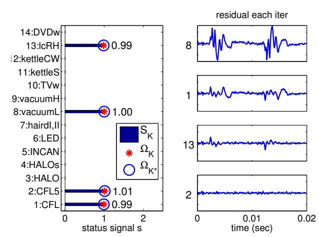

(a) $\tilde{\mathbf{i}}'$ 10 kHz, $\mathbf{\Phi}$ **Nyquist**

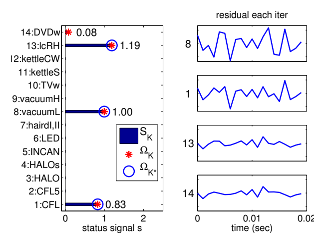

(b) $\mathbf{i}'_{\mathrm{m}}$ 1 kHz, $\mathbf{\Phi}$ **subs**

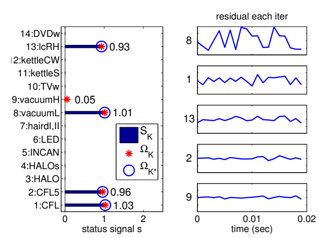

(c) $\mathbf{i}'_{\mathrm{m}}$ 1 kHz, $\mathbf{\Phi}$ **randg**

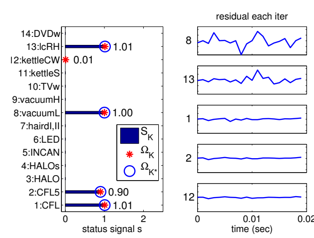

(d) $\mathbf{i}'_{\mathrm{m}}$ 1 kHz, $\mathbf{\Phi}$ **rands**

Figure 11. Appliance identification (A-OMP) with the compressed signal. Measurement $\tilde{\mathbf{i}}'$ with [1 2 8 13] 'on'.

Figure 11 gives the appliance identification results of applying A-OMP on the signal sampled/compressed by different $\mathbf{\Phi}$'s. As shown in (11a), using the non-compressed signal we correctly identify the 'on' appliances to be [1 2 8 13]. As shown in (11c) and (11d), we can still achieve correct appliance identification using the signal compressed by random sampling ($\mathbf{\Phi}$ **randg** or $\mathbf{\Phi}$ **rands**). While in (11b), using the signal compressed by conventional sub-sampling, the 'on' appliance 2 (CFL5) is not identified. The conventional sub-sampling at 1 kHz destroys the high-frequency components outside the 1 kHz band and causes too much information loss. The random sampling at 1 kHz maintains the essential information with high probability and ensures perfect recovery of $\mathbf{s}'$.

The on-line monitoring can employ a two-step approach. Let τ_1 be an initial time instant when we do not know the on/off status of any appliances, and τ_2 be a time instant shortly after τ_1. In between τ_1 and τ_2, some (at most K_0) appliances change their status, which triggers a simple event detector based on the total power variation. Step 1) **Initial detection** at τ_1: We use Nyquist-rate sampling and estimate $\mathbf{s}_{\tau_1}$ from $\tilde{\mathbf{i}}_{\tau_1}$ (10 kHz). Step 2) **Differential detection** at τ_2 (and at any later time instants): We use compressive sampling and estimate $\mathbf{s}'$ from the compressed difference signal $\mathbf{i}'_{\mathrm{m}}$ (1 kHz). Then $\mathbf{s}_{\tau_2}$ is given by $\mathbf{s}_{\tau_1} + \mathbf{s}'$. If we estimate $\mathbf{s}_{\tau_2}$ directly from the compressed samples at τ_2, then $\mathbf{s}_{\tau_2}$ may not be sparse enough to allow much compression.

4 Simulation Results

The performance of the appliance identification using compressive sampling is evaluated by Monte Carlo simulation. We use the 14 signatures as mentioned in Section 3. In each simulation round, 4 randomly selected appliances are simultaneously on, and the total current is corrupted by an additive white Gaussian noise of zero-mean and variance of 0.01. Given the Nyquist-rate signal of 10 kHz, we consider the compressed signal of 1 kHz and 0.5 kHz using the three compression methods 'subs', 'rands', and 'randg' as explained in Section 3.5. The disaggregation algorithm is A-OMP. For each scenario with a certain compression rate and a compression method, we perform $N_{\text{sim}} = 10^4$ simulation rounds. The error rate of a particular appliance is defined by $N_{\text{err}}/N_{\text{sim}}$, where N_{err} is the number of times when the appliance's on/off status is wrongly identified. We obtain the total error rate by averaging over all the appliances. The results are shown in the following table.

Table 3. Error rates of different compression methods.

	subs	rands	randg
1 kHz	5.3%	3.6%	1.8%
0.5 kHz	25.7%	16.6%	11%

For the Nyquist-rate signal of 10 kHz, the error rate is 0. For the compressed signal of 1 kHz, the conventional sub-sampling 'subs' gives the highest error rate of 5.3%, and the two random sampling methods give lower error rates, where 'randg' gives the lowest error rate of 1.8%. Similar conclusion holds for the more heavily compressed signal of 0.5 kHz.

5 Conclusions

We have proposed a NALM solution to estimate the individual appliance's on/off status from the measured current of the total load. We exploited the sparsity of the current signal given by SCP, which allows us to sample and compress the measured current without degrading much the appliance identification performance. The problem of identifying the on/off status of appliances is formulated as a sparse reconstruction problem, which can be solved using the proposed A-MP/A-OMP algorithms. We conducted experiments using 12 household appliances to verify the proposed NALM solution. Our simulation results shown that compression via random sampling achieves lower error rates than conventional sub-sampling.

References

[1] G. W. Hart, "Nonintrusive Appliance Load Monitoring," *Proc. IEEE*, pp. 1870-1891, Dec. 1992.

[2] D. Donoho, "Compressed sensing", *IEEE Trans. on Information Theory*, pp. 1289-1306, Apr. 2006.

[3] C. Laughman, K. Lee, R. Cox, S. Shaw, S. Leeb, L. Norford and P. Armstrong, "Power signature analysis", *IEEE Power and Energy Magazine*, pp. 56-63, Mar/Apr 2003.

[4] J. Laska, S. Kirolos, Y. Massoud, R. Baraniuk, A. Gilbert, M. Iwen, and M. Strauss, "Random sampling for analog-to-information conversion of wideband signals," *IEEE Dallas Circuits and Systems Workshop*, pp. 119-122, Oct. 2006.

[5] K. Suzuki, S. Inagaki, T. Suzuki, H. Nakamura and K. Ito, "Nonintrusive appliance load monitoring based on integer programming", *SICE Annual Conference*, pp. 2742-2747, 2008.

[6] J. Tropp and A. Gilbert, "Signal recovery from random meaurements via orthogonal matching pursuit", *IEEE Trans. on Information Theory*, pp. 4655-4666, Dec. 2007.